

## Characterisation of a continuous blender: Impact of physical properties on mass holdup behaviour

Hikaru Graeme Jolliffe<sup>a</sup>, Maria A. Velazco-Roa<sup>a</sup>, Luis Martin de Juan<sup>b</sup>, Martin Prostedny<sup>a</sup>, Carlota Mendez Torrecillas<sup>a</sup>, Gavin Reynolds<sup>b</sup>, Deborah McElhone<sup>c</sup>, John Robertson<sup>a,\*</sup>

<sup>a</sup> CMAC, University of Strathclyde, 99 George Street, G1 1RD, Glasgow, UK

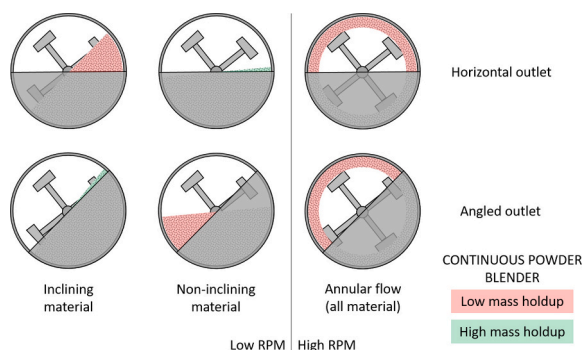
<sup>b</sup> Oral Product Development, PT&D, Operations, AstraZeneca UK Limited, Charter Way, Macclesfield SK10 2NA, UK

<sup>c</sup> CPI's Medicines Manufacturing Innovation Centre, 1 Netherton Square, Paisley, Glasgow PA3 2EF, UK

### HIGHLIGHTS

- Interaction between equipment geometry and material properties highlighted.
- Opposing behaviour of high-density free-flowing material and low-density cohesive material.
- Impact on mass hold up behaviour of process settings and material properties (equipment configuration dependant).
- Impact on continuous direct compression operation.

### GRAPHICAL ABSTRACT



### ARTICLE INFO

#### Keywords:

Continuous powder blending  
Continuous direct compression

### ABSTRACT

Continuous blenders are a key unit operation in Continuous Direct Compaction, a route to solid oral dosage forms that is receiving significant interest. Mass holdup in these blenders is a crucial variable; understanding how it is influenced by material properties, equipment configuration and process settings is key. The present work evaluated a Gericke GCM-450 blender for range of outlet weir aperture geometries (angled or horizontal), material properties (pure components and blends) and process settings (throughput and impeller speed). Results show opposing mass holdup behaviour depending on weir choice, material density and flowability, likely linked to the propensity of the material to form an inclined powder surface that matches – or does not – the chosen weir geometry. The present work underscores the need for fundamental process phenomena understanding, especially when insight is sought for how blender performance varies across multiple dimensions (throughput, impeller speed, material properties) and discrete equipment choices (weir geometry).

\* Corresponding author.

E-mail address: [j.robertson@strath.ac.uk](mailto:j.robertson@strath.ac.uk) (J. Robertson).

<https://doi.org/10.1016/j.powtec.2024.120440>

Received 12 September 2024; Received in revised form 7 November 2024; Accepted 8 November 2024

Available online 12 November 2024

0032-5910/© 2024 The Authors. Published by Elsevier B.V. This is an open access article under the CC BY license (<http://creativecommons.org/licenses/by/4.0/>).

## 1. Introduction

Interest in continuous manufacturing in the pharmaceutical industry for both drug substance [3] and drug product has increased considerably in the last decade [6,19]. This has been possible largely due to the reframe of regulatory bodies such as the United States Food and Drug Administration [25,26] to encourage within the pharmaceutical industry the use and implementation of new technologies (e.g. process analytical technology, PAT) and new methodologies (e.g. quality by design, QbD) that are based on the success of increasing process efficiency in other, more mature industry sectors including food, fertilisers and petrochemicals.

Various processing routes for the continuous manufacturing of oral dose form drug products are available, with common ones being continuous granulation, roller compaction and continuous direct compression (CDC). Due to its simplicity, as it only involves three key unit operations of feeding, blending and tablet compression/compaction, CDC is often preferred where possible by the pharmaceutical industry, and significant research efforts have been put towards the further development of this manufacturing route.

Efficient continuous blending is required to minimise powder segregation and agglomeration during production. Compared to batch blending, continuous blending offers some advantages such as a smaller equipment footprint, easier process scale-up, less materials handling, and greater scope for process control [13]. However, limitations include high initial CAPEX costs, difficulties with handling extremely small quantities of material, and process flexibility [23,27].

The concept of Residence Time Distribution (RTD) – a methodology originally developed for continuous flow reactors – has been used to describe the performance of the continuous powder blenders [4]. It provides information about the duration (age, or mean residence time), and distribution of durations that the given particles of solid material stay within the blender system. It allows a description of the macro-mixing behaviour, and up to a certain extent an understanding of micro-mixing [12]. The RTD curve (also known as the exit age distribution curve  $E$ ) and the mean residence time  $\tau$  can be computed by normalizing a continuously evolving concentration ( $C$ ) of a known material by [5,16]:

$$RTD = E(t) = \frac{C(t)}{\int_0^{\infty} C(t)} \quad (1)$$

$$\tau = \int_0^{\infty} tE(t)dt \quad (2)$$

Experimentally, RTD profiles can be obtained by dosing a small quantity of tracer material (in a ‘pulse’ experiment) or by causing a step-change in tracer concentration, with the caveat that such changes should not modify the bulk flow behaviour of the system [9,10]. RTD information about the system can be determined by comparing the outlet concentration profile to the inlet concentration profile. A variety of data-driven models exist to describe the RTD profiles as functions of parameters (including the mean residence time), with the most common approaches in the literature being Axial Dispersion (AD) and nCSTR models [9,11].

Mean residence time can be coarsely estimated using mass throughput and mass holdup, denoted here by  $\tau_{\text{mass}}$ :

$$\tau_{\text{mass}}(t) = \frac{M(t)}{\dot{m}(t)} \quad (3)$$

where  $M(t)$  is the mass holdup, and  $\dot{m}(t)$  is the throughput. Understanding and control of the mass holdup is key towards ensuring adequate residence times.

Many works to date have shown that, for a given formulation, mean residence times and RTD profiles vary depending on blender operating conditions and design (such as blade angle and outlet weir aperture size

and shape) [15,17,20,27,29]. While the impact of blender design has been significantly explored, the effect of powder properties on continuous blending performance is still not fully understood due to the large number of variables that can affect the blending process.

Portillo and co-workers experimentally evaluated continuous GEA blenders, finding that the impeller speed and blender angle have a significant effect on the RTD, and finding that cohesion also had an impact in larger blenders [20–22]. Similar behaviour is also reported for GCM 250 blenders with 45° outlet weirs – work by Dubey and co-workers (using experiments, DEM, and periodic slice simulations) showed how mean residence time decreases with increasing impeller speed and increasing throughput (although with increasing impeller speed the impact of throughput gradually lessens) [7,8,12].

Vanarase and co-workers, similarly using a GCM 250 blender, also elucidated this impact of throughput and impeller speed [27]. Additionally, the impact on mass holdup and how it responds different outlet weir angles was reported in detail. Mass holdup responds in a similar manner to mean residence time, decreasing with increasing impeller speed and increasing with mass throughput (with the latter trend significantly attenuated by high impeller speeds). It was reported that the use of angled weirs (in particular one inclined at 45°) results in higher mass holdup values, even when the powder is substantially fluidised at high impeller speeds, with the stated reason being that the powder bed forms an incline as a result of blade rotation, and that when this matches the weir angle, greater mass is retained within the blender. Subsequent using work using the data-driven approach of Partial Least Squares (PLS) multivariate statistical regression illustrated the impact of bulk density, where greater densities lead to higher mass holdup when impeller speeds are low (and there is little fluidisation), and where high impeller speeds (and a high degree of fluidisation) mean there is minimal impact from density [28]. The use of PLS in with another type of horizontal blender from Fette Compacting indicated that the only way to change mass holdup was to alter process settings or impeller configuration, that the use of weir plates had no significant impact, and that material properties did not meaningfully affect holdup mass [1,2].

Data-driven models can have great utility in identifying possible trends in complex multivariate systems, and recently, Artificial Intelligence (AI) and Machine Learning (ML) have been used to explore the performance of continuous blenders. Jones-Salkey and co-workers (2024) used three AI/ML models to characterise an inclined GEA blender. Mass throughput, impeller speed, blender configuration, and that material properties (specifically, wall friction angle) are identified as factors to predict the fill level (and hence mass holdup).

Understanding the interaction how the mass holdup responds to key process parameters, design parameters and material properties is key towards understanding other unit operation aspects that are known to be related to mean residence time, such as content uniformity [18]. The present work sets out to elucidate key process phenomena (mass holdup, mean residence time) in a Gericke GCM 450 continuous blender, and explores the impact of mass throughput, blender speed, outlet weir angle and material properties (both pure components and blends were used). In particular, it explores the influence on mass holdup of the two weirs settings (either horizontal or 45°) that results in varying mass holdup depending on the material properties of the powder being blended. Data-driven modelling (PLS) was used to quantify the observed trends and highlight those conditions that do not follow reported literature behaviour for continuous blenders.

## 2. Methodology

### 2.1. Equipment

A GCM 450 continuous horizontal tubular blender (Gericke, Switzerland) placed on a digital load cell was used for the tests (Fig. 1). Materials are fed into the inlet port from the top by a QT20 feeder (Coperion K-Tron, Germany); the blender was lifted to a higher position

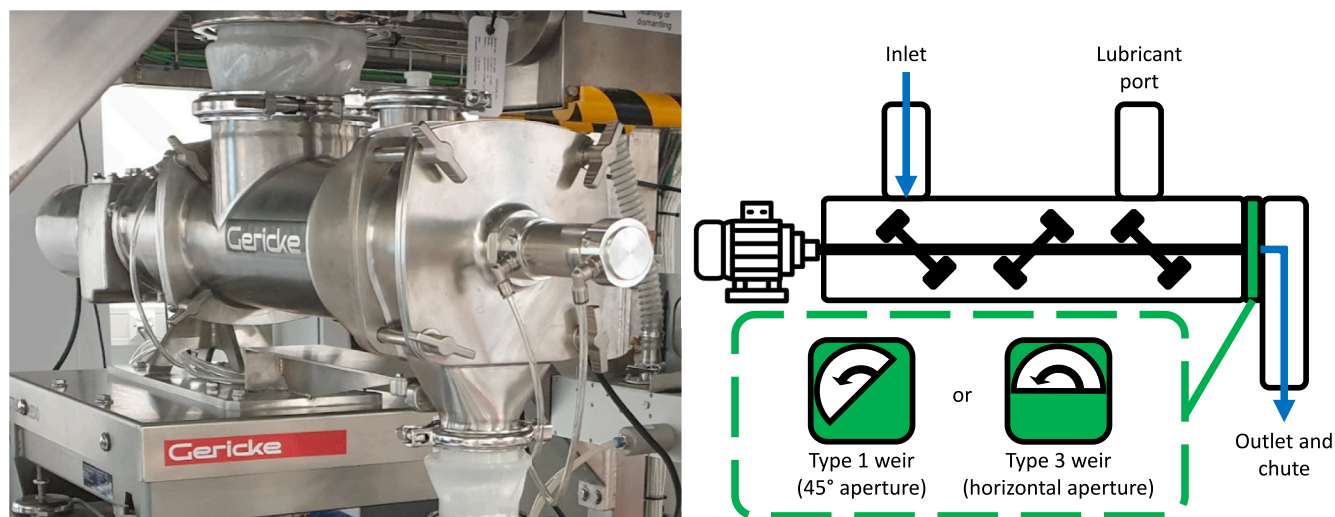


**Fig. 1.** The GCM 450 continuous blender. One of two outlet weirs is installed during operation: a weir plate with a 45° aperture (type 1), or a weir plate with a horizontal aperture (type 3); arrows in weir graphic indicate direction of blade rotation (counterclockwise when looking along the axis from the outlet). No lubricant was used in the data presented in this work.

to reduce the length of the pipe between the feeder and the blender inlet. Rotating paddles inside the blender mixing chamber drive the blending. At the end of the processing chamber there was an exchangeable weir plate with different aperture geometry (Fig. 1). Weir choice is intended as a quick way to affect mass holdup. The blender has an operating range from 55 to 181 RPM. The maximum capacity of the chamber is approximately 7.9 L. The blender was equipped with a start-up valve, for reducing product lost during start-up until the blender reached steady-state conditions.

## 2.2. Materials

The materials used in this study consist of dicalcium phosphate anhydrous (DCPA, EMCOMPRESS® Anhydrous, JRS PHARMA), crystalline lactose (SuperTab® 11 SD, DFE Pharma), microcrystalline cellulose (MCC; Avicel® PH-101, Avicel® PH-102 and Avicel® PH-200, DuPont; Pharmacel® 102, DFE Pharma) and powder grade acetaminophen (APAP, Mallinckrodt).

Three different blends were prepared to model typical pharmaceutical formulations and to achieve a wide range of material properties. Two categories of blends were used: those that consist of a mix of lactose (SuperTab® 11 SD), microcrystalline cellulose (Pharmacel® 102) and powdered APAP; and those that include DCPA, Pharmacel® 102, and powdered APAP.

## 2.3. Material characterisation

All the materials used in this study were characterized to obtain particle size, density, and flow properties. Particle size distribution was measured in triplicate by dynamic image analysis (QICPIC with RODOS/L dispenser, Sympatec GmbH). Bulk and tapped density were measured in triplicate using a Quantachrome Auto Tap as per British Pharmacopoeia method [24]. True density was measured in a Quantachrome Pycnometer. Major Principal Stress (MPS), Unconfined Failure Strength (UFS) and Flow Function Coefficient (FFC) were measured on Brookfield PFT at consolidation end points of 1.06 kPa, 1.68 kPa, 2.66 kPa, 4.2 kPa, and 6.63 kPa for single materials and at 1.06 kPa for blends (1.06 kPa values used in PLS modelling). Measured material properties for pure materials are summarised in Table 1. For blends, characterisations were frequently performed each run, and these were used in PLS modelling for each relevant data point; averaged blend properties are given in Table 2.

## 2.4. Mass holdup tests

The mass holdup tests were performed on single materials and different blends at different process conditions using different weir types. APAP was used in a 10 % formulation (Table 2) as this has been often used as a model formulation in the literature [13,18]. The conditions are presented in Table 3 and Table 4.

Some repeats were done for the single materials. The feeder feed rates, blender impeller speed, and blender mass throughput and net

**Table 1**

Single material physical properties. In blends, Pharmacel® 102 was used instead of Avicel® PH-102. Only properties used in PLS modelling shown.

Single components	Material	$\rho_{\text{bulk}}$ (g/cm <sup>3</sup> )	$\rho_{\text{tapped}}$ (g/cm <sup>3</sup> )	$\rho_{\text{true}}$ (g/cm <sup>3</sup> )	$d_{10}$ (μm)	$d_{50}$ (μm)	$d_{90}$ (μm)	MPS (kPa)	UFS (kPa)	C (kPa)	$\phi'$ (°)	FFC (–)
Avicel® PH-101	Microcrystalline cellulose	0.312	0.420	1.57	37	74	121	2.17	0.66	0.17	43.5	3
Avicel® PH-102	Microcrystalline cellulose	0.352	0.438	1.57	45	121	237	1.94	0.44	0.12	39.3	4
Avicel® PH-200	Microcrystalline cellulose	0.343	0.420	1.57	58	146	283	1.80	0.27	0.08	35.0	7
SuperTab® 11 SD	Crystalline lactose	0.605	0.714	1.54	53	137	240	1.85	0.30	0.08	36.0	6
EMCOMPRESS® Anhydrous (DCPA)	Dicalcium phosphate anhydrous	0.740	0.870	2.87	78	175	269	1.81	0.15	0.04	36.2	13
Pharmacel® 102	Microcrystalline cellulose	0.361	0.485	1.54	34	96	223	1.92	0.42	0.11	39.8	5
APAP powdered	Paracetamol	0.343	0.553	1.18	23	70	189	2.17	1.32	0.37	51.4	2

**Table 2**

Blend mixture physical properties (average values). Only properties used in PLS modelling shown.

Blend	Composition (weight %)	Bulk density (g/cm <sup>3</sup> )	Tap density (g/cm <sup>3</sup> )	d <sub>10</sub> (μm)	d <sub>50</sub> (μm)	d <sub>90</sub> (μm)	MPS (kPa)	UFS (kPa)	C (kPa)	φ' (°)	FFC (–)
1	SuperTab® 11 SD (70 %)	0.56	0.68	34	111	223	1.87	0.45	0.13	38	4
	Pharmacel® 102 (20 %)										
	APAP powder (10 %)										
2	SuperTab® 11 SD (20 %)	0.43	0.54	28	87	219	1.94	0.54	0.15	41	4
	Pharmacel® 102 (70 %)										
	APAP powder (10 %)										
3	DCPA (39 %)	0.52	0.66	33	103	231	1.93	0.51	0.14	41	4
	Pharmacel® 102 (51 %)										
	APAP powder (10 %)										

**Table 3**

Mass holdup test blender conditions for single components.

Pure component	Weir Type	Throughput kg/h	Blender Speed RPM
DCPA			
SuperTab® 11 SD			
Avicel® PH-101	1, 3	10, 20, 30, 40	60, 85, 110, 180
Avicel® PH-102			
Avicel® PH-200			

**Table 4**

Mass holdup test blender conditions for blends.

Blend	Composition (weight %)	Weir	Throughput (kg/h)	Blender speed (RPM)
1	SuperTab® 11 SD (70 %)	1, 3	10, 20, 30, 40	60, 85, 110, 180
	Pharmacel® 102 (20 %)			
	APAP powder (10 %)			
2	SuperTab® 11 SD (20 %)	1, 3	10, 20, 30, 40	60, 85, 110, 180
	Pharmacel® 102 (70 %)			
	APAP powder (10 %)			
3	DCPA (39 %)	1, 3	10, 20, 40	60, 85, 110, 180
	Pharmacel® 102 (51 %)			
	APAP powder (10 %)			

weight were monitored and collected using PharmaMV® Real-Time. Prior to starting the tests the blender weight was calibrated with the corresponding weir in place. For each speed, throughput and weir, the equipment was required to reach a steady blender weight ( $\pm 5$ –6 g blender change) before conditions were considered steady state. The data was collected for 5 to 10 min after the steady state condition was reached.

### 3. Results and discussions

Mass holdup data has been collected for the blender running at steady state at various throughputs, impeller speeds, weir choices (horizontal or angled aperture), and material properties (various pure materials of differing material properties, and multiple blends also covering a range of material properties).

#### 3.1. Pure component mass holdup and mean residence time

The effect of the throughput and the impeller speed on the mass holdup in the blender was evaluated using both weirs. For pure components evaluated in this study, mass holdup increased with throughput at intermediate blender speeds (85 RPM, Fig. 2). For Avicel® PH-101

(Fig. 2A), Avicel® PH-102 (Fig. 2B) and Avicel® PH-200 (Fig. 2C) the throughput appeared to increase following a convex from above trend, although for Avicel® PH-200 there was comparatively smaller impact of weir choice. For these materials, the mass holdup when the horizontal weir 3 is used exhibit higher mass holdup than when the angled weir 1 is used. However, SuperTab® 11 SD and DCPA (Fig. 2D and E, respectively) showed the opposite – the mass holdup for angled weir is higher than for the horizontal weir, and holdup generally appeared concave from above, at least within the mass throughput range explored (10–40 kg/h). For the lower density, low FFC materials (Avicel® PH-101 and PH-102, Fig. 2A and B), the horizontal weir (3) consistently resulted in higher mass holdup regardless of throughput, whereas for the other materials, the impact of weir (aside from the opposite behaviour of SuperTab® 11 SD and DCPA) only becomes evident at higher throughputs *i.e.* at lower throughputs, the mass holdup is similar for both weirs (Fig. 2C–E).

Whilst conducted with a smaller scale blender, literature suggests that an angled weir should result in higher mass holdup [27], consistent with the observed behaviour of SuperTab® 11 SD and DCPA, but not of the comparatively cohesive Avicel® materials (smaller particle size and/or smaller FFC, Fig. 2; a common definition of flowability uses FFC, Table 5). The least cohesive Avicel® (PH-200) shows intermediate behaviour, with similar mass holdup from both weirs, although it is still slightly higher with the horizontal weir 3 (Fig. 2C); while it has a FFC value classed as easy flowing, it has lower bulk density.

The effect of the impeller speed on the mass holdup was also evaluated for both angled and horizontal weirs (Fig. 3), and shows similar trends to mass holdup as a function of throughput (Fig. 2); the angled weir 1 results in higher mass holdup for free flowing and easy flowing materials that have higher bulk densities (Fig. 3D and E, Table 5), with the opposite true for the other materials (Fig. 3A and B). Also, as impeller speeds increase, mass holdup decreases, which is expected and frequently reported in the literature for various types of continuous blender [1,15,17,27], and mass holdup gradually becomes independent of weir choice at high impeller speeds, likely due to fluidisation of the powder as inertial forces overcome gravitational forces. Of note is that the impact of low impeller speed is much more pronounced for free flowing and easy flowing materials in the angled weir, with mass holdup at 60 RPM over three times that of the horizontal weir (Fig. 3D and E). This exponential decay shape for mass holdup in the angled weir with increasing impeller speed also appears to be present with Avicel®, although it is less pronounced than for SuperTab® 11 SD and DCPA, and as mentioned is in lower than the horizontal weir as opposed to higher (Fig. 3A–C).

Another difference with the more poorly-flowing (cohesive) materials is that, similar to when mass holdup is plotted against throughput, when plotted against impeller speed the horizontal weir influences the shape of the relationship (*i.e.* whether concave or convex from above); Avicel® PH-101, PH-102 and PH-200 appeared linear if not convex from above. At the lowest blender speeds highest throughput it appears that the maximum holdup depends on the physical properties of the material

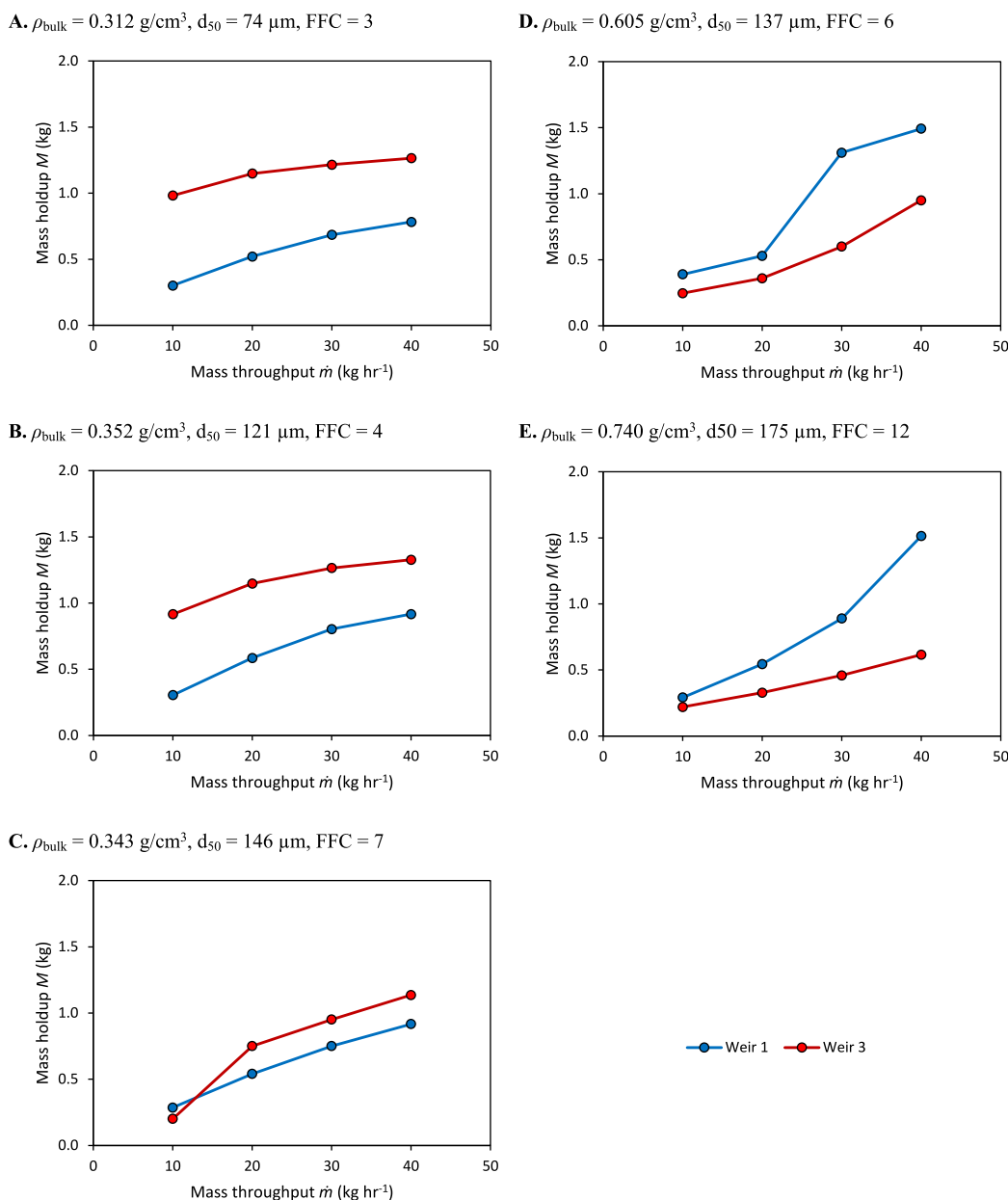


Fig. 2. Blender mass holdup as function of throughput at constant blender speed (85 RPM) for weir (1) and horizontal weir (3). A: Avicel® PH-101, B: Avicel® PH-102, C: Avicel® PH-200, D: SuperTab® 11 SD, E: DCPA.

**Table 5**  
Powder flowability classification [14].

Flow function coefficient	Type of flow
10 < FFC	Free flowing
4 < FFC < 10	Easy flowing
2 < FFC < 4	Cohesive
FFC < 2	Very cohesive (non-flowing)

and not only on the geometry of the weir used as reported in the literature [27].

Whether compared against throughput or impeller speed, Avicel® PH-101 and PH-102 (Fig. 2A–B, Fig. 3A–B) showed a higher mass holdup for the horizontal weir than for the angled weir; these two materials have the relatively low bulk densities (0.312 g/cm<sup>3</sup> and 0.352 g/cm<sup>3</sup>, respectively) and FFC values classified as cohesive (Table 5) compared

to the free and easy flowing materials that show responses similar to that reported for angled and horizontal weir mass holdup [27]. While Avicel® PH-200 has a similar bulk density (0.343 g/cm<sup>3</sup>) it has better flowability (FFC = 7), and mass holdup appeared to be independent from the weir type as the trends for both angled and horizontal weir appeared to overlap (Fig. 2C, Fig. 3C).

The effect of the throughput and impeller speed on the mean residence time (Eq. (3)) was also evaluated for the pure components (Fig. 4A–B). Calculated from mass holdup and throughput (Eq. (3)), no clear trends were observed for mean residence time as a function of throughput with the angled weir (Fig. 4A), aside from the distinctly different behaviour between the cohesive Avicel® materials (PH-101 and PH-102) and the other materials (Avicel® PH-200, SuperTab® 11 SD, DCPA). These two Avicel® materials had markedly higher mean residence time at lower throughput that gradually lowered with increasing throughput, while the other materials showed little change in



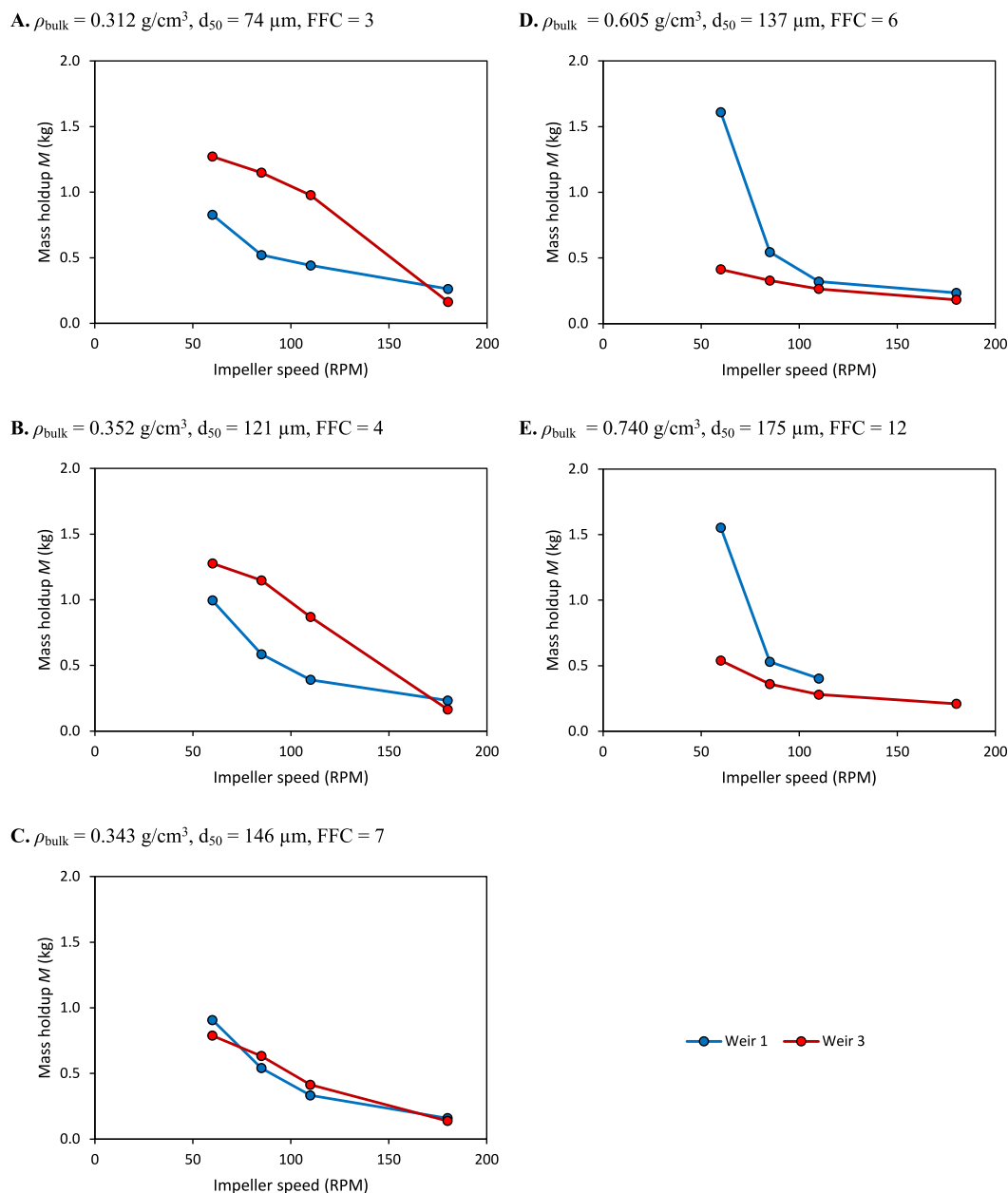


**Fig. 3.** Blender mass holdup as function of impeller speed at constant throughput (20 kg/h) for angled weir (1) and horizontal weir (3). A: Avicel® PH-101, B: Avicel® PH-102. C: Avicel® PH-200, D: SuperTab® 11 SD, and E: DCPA.

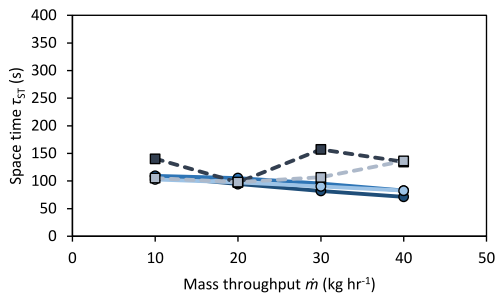
mean residence time as a function of throughput (Fig. 4B). In general mean residence time will decrease as a result of increasing throughput [7,8,20,27], although in some blenders the opposite can occur at extremely high blender speeds [22].

The trends of mean residence time against impeller speed are more consistent. In the angled weir, the free and easy flowing SuperTab® 11 SD and DCPA show higher values than other materials, with the opposing behaviour in the horizontal weir (Fig. 4C–D), although this is only the case for lowest RPM values in the angled weir, with identical response from all materials in the angled weir at higher RPM values (Fig. 4C). Also, the datasets are generally more linear in the horizontal weir, as seen with throughput (Fig. 2, Fig. 3).

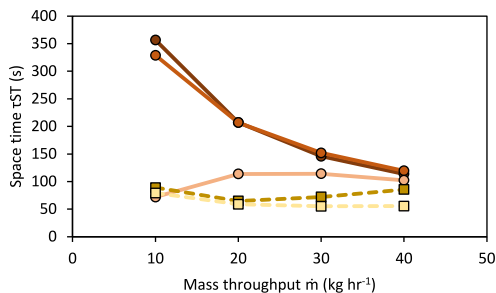
### 3.2. PLS modelling - effect of material properties on the mass holdup

Observations indicate that at low RPM, use of the angled weirs leads to higher mass holdup for some materials (Avicel® PH-101, PH-102), while horizontal weirs lead to higher mass holdup for other materials (SuperTab® 11 SD, DCPA), and that at high RPM the properties of the materials do not matter with holdup being largely governed by impeller speed and throughput. Vanarase and Muzzio [27] have previously reported that outlet weir geometries with an inclined aperture lead to higher mass holdup, albeit in a smaller scale blender than the GCM 450 used in the present work; furthermore, the study by Vanarase and Muzzio [27] reported only that use of horizontal weir resulted in lower mass hold up whereas the present work observed cases where the horizontal weir could also result in higher mass holdup (depending on the material).

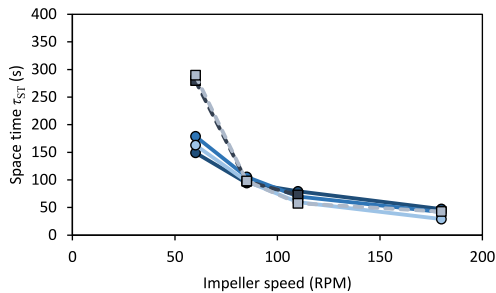
A. Angled weir – constant impeller speed (85 RPM)



B. Horizontal weir – constant impeller speed (85 RPM)



C. Angled weir – constant throughput (20 kg/h)



D. Horizontal weir – constant throughput (20 kg/h)

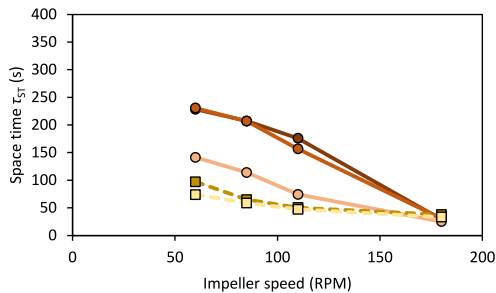


Fig. 4. Mean residence time as a function of material properties (via different single materials Avicel® PH-101, PH-102, and PH-200; SuperTab® 11 SD; and DCPA), mass throughput (A,B) and impeller speed (C,D), for two different weirs (angled or horizontal, Fig. 1). Constant impeller speed conditions are at 85 RPM, and constant throughput conditions are at 20 kg/h.

A visualisation of these behaviour categories – inclining and non-inclining material – is given in Fig. 5. Expanding on literature observations of outlet weir geometry effect on mass holdup [27], and to quantify what factors contribute to material behaving in one manner or the other (higher mass holdup with angled or horizontal weir), Partial Least Squares / Projection to Latent Structures (PLS) modelling was used.

Pure components (Avicel® PH-101, PH-102, PH-200; SuperTab® 11 SD; EMCOMPRESS® Anhydrous DCPA; Table 1) were used to regress and train the PLS model. Blends (1, 2, and 3; Table 2) were used as test data. Predictors evaluated for PLS modelling were material properties (bulk density; particle size measurements of  $d_{10}$ ,  $d_{50}$  and  $d_{90}$ ; major principal stress at 1.06 kPa consolidation end point; unconfined failure strength at 1.06 kPa consolidation end point; cohesion at 1.06 kPa consolidation end point; effective angle of internal friction at 1.06 kPa consolidation end point; and FFC at 1.06 kPa consolidation end point), alongside throughput and impeller speed. Using the full set of material properties showed that many were highly correlated, and in general two principal components were enough to explain most of the variance in the response of mass holdup. This work uses a main set of predictors (throughput, impeller speed, bulk density, cohesion, and FFC) and two principal components, and figures relating to PLS results using all predictors are provided in the Supplementary Information; use of additional predictors did not increase the response variance explained and obscured the contributions of some key predictors, and there were rapidly diminishing returns beyond using two principal components. Furthermore, applying PLS for responses other than mass holdup (*i.e.* mean residence time) did not result in meaningful trends, similar to work of Bekaert et al. [1] and expected based on the lack of clear trends that would make PLS models less responsive (Fig. 4). Data has been

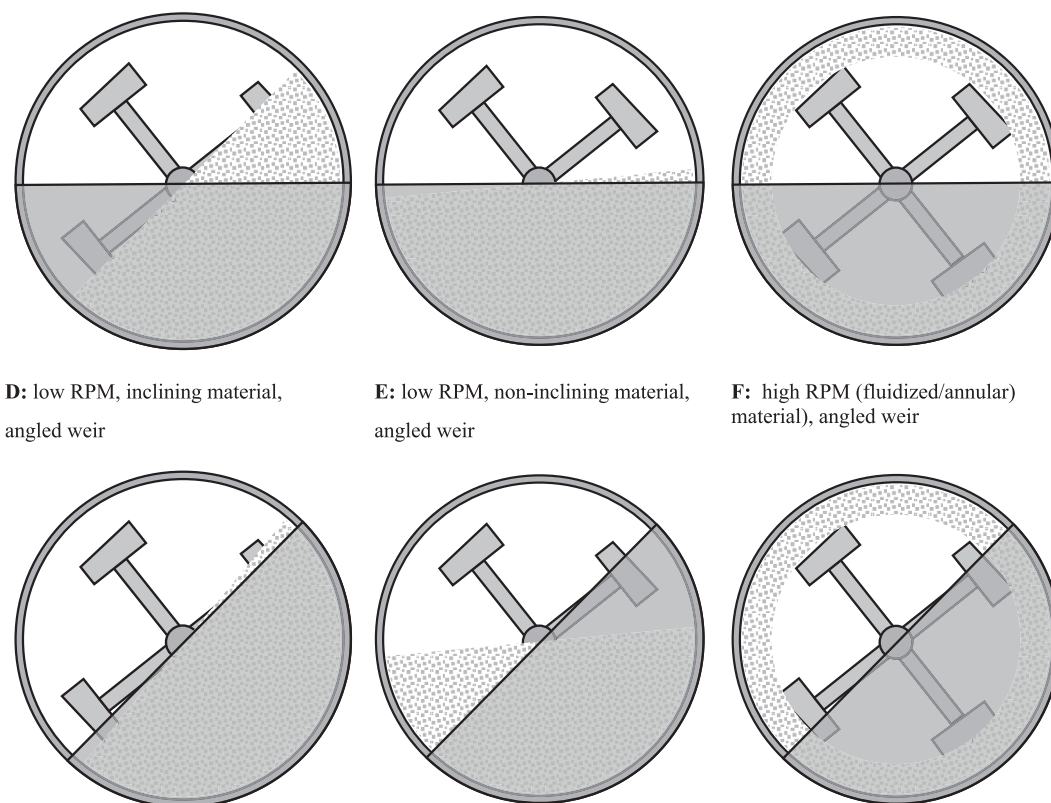
mean centered and standardised using z-scores, with log transformations used to ensure there are no negative values.

Each weir was treated separately – PLS performed on a single overall dataset obscured differences between the two weirs (aside from highlighting that weir choice is meaningful). In both cases, as stated two principal components were sufficient to explain as much variance as practical, with rapidly diminishing returns beyond that number (Table 6); two components have been used in the present work.

The scores plot for each weir shows clear clustering by material (Fig. 6A and B). Avicel® PH-101 (cohesive) is in one quadrant while DCPA and SuperTab® 11 SD (free and easy flowing) are located in the opposite quadrant. This is the same for both weirs. Looking at the loadings biplots (Fig. 6C and D), it can be seen how this clustering is informed by the different material properties. Also evident are how the spread of scores of each material align with throughput and impeller speed in the biplot, and how the latter two align with the response (mass holdup).

Whilst evident without needing PLS, the PLS results show the strong relevance of throughput to increasing holdup, and impeller speed to decreasing it (throughput in the same quadrant as holdup, and impeller speed in the opposite quadrant). This is well-established behaviour for most continuous blenders [1,15,27]. For the other predictors – the material properties – the impact is less clear with the vectors having angles that approach orthogonal ( $10^{\circ}$ – $15^{\circ}$  from orthogonal). It is nevertheless clear from the data from each weir used in the present work that material properties (and weir choice) impact mass holdup, which diverges from some reported blender observations of weir use and material properties not having a significant effect [1] but is consistent with others [15].

The impact of the predictors can also be explored via predictor



**D:** low RPM, inclining material, angled weir

**E:** low RPM, non-inclining material, angled weir

**F:** high RPM (fluidized/annular material), angled weir

**Fig. 5.** Illustrative examples of potential phenomena at blender exit aperture. A: low RPM, impeller can easily convey material over a horizontal weir due to if material has a tendency to incline. B: low RPM, impeller has more difficulty conveying material over horizontal aperture due to good material flowability. C: material easily conveyed over horizontal weir due to high RPM and centrifugal forces, regardless of whether material would incline or not at low RPM. D: low RPM, impeller struggles to convey an inclining material over an angled weir that has a similar angle to the bulk material surface. E: low RPM, impellers easily convey non-inclining material over an angled weir as the material easily flows to the lower portions of the blender. F: material easily conveyed over angled weir due to high RPM and centrifugal forces, regardless of whether material would incline or not at low RPM.

**Table 6**

Additional explained variance in the response variable (mass holdup) from increasing the number of principal components. Two principal components were used in this work. Predictors are mass throughput, impeller speed, bulk density, cohesion, and FFC.

Number of principal components	Angled weir	Horizontal weir
1	75.1 %	66.3 %
2	7.3 %	14.1 %
3	0.9 %	0.4 %
4	0.2 %	0.4 %

coefficients and Variable Importance in Projection (VIP) scores (Fig. 7); the former show the estimated coefficients of the PLS regression model for each predictor variable (representing the relationship between the predictors and response variable), while the latter is an overall view of the importance of each predictor considering all principal components, and includes weighting according to the amount of response variance explained by each component. Similar insight is gained as for the biplots (Fig. 6C, D): throughput and impeller speed are by far the most important variables. The predictors with a positive impact on holdup tend to change depending on weir. In the angled weir, bulk density has a positive coefficient, and cohesion and FFC have comparatively little impact. Meanwhile, in the horizontal weir, the opposite is true, with cohesion having a much more positive coefficient, bulk density a similarly negative coefficient, and FFC also has a negative coefficient (Fig. 7A and B); with the horizontal weir cohesive material properties are more relevant than with the angled weir. Looking at the overall importance of the predictors in the VIP scores, the importance of impeller speed and

throughput are reiterated, and the greater importance of material properties when the horizontal weir is used is further underscored (Fig. 7C and D).

Parity plots for the pure components – *i.e.* data used to regress the PLS models – shows that the two PLS models (one for each weir) are generally similar: more accurate regression (data points closer to the parity line) at lower mass holdups, with it tending to diverge at higher mass holdup (Fig. 8A and B); comparing the two weirs, data for the horizontal weir shows a marginally improved regression ( $R^2 = 0.785$ , RMSE = 0.182 kg, Fig. 8B) than the angled weir ( $R^2 = 0.701$ , RMSE = 0.229 kg, Fig. 8A).

Testing the PLS models with data for the blends shows some notable trends (Fig. 8C and D). As might be expected for test data, accuracy metrics are lower than the training set (angled weir  $R^2$  and RMSE of 0.479 and 0.233 kg, respectively; horizontal weir  $R^2$  and RMSE of 0.622 and 0.394 kg, respectively). Whilst challenging to draw definitive conclusions, both the test sets for the weirs appear to show a trend of slight overprediction (angled weir) and underprediction (horizontal weir), and this could be linked to the opposing effects of material properties identified by the PLS analysis (particularly bulk density and cohesion, Fig. 7).

Also, the test data for the angled weir are less scattered than for the horizontal weir. A potential cause for the different degrees of scattering is the fact with the angled weir material properties appear less relevant relative to the process conditions of throughput and impeller speed (Fig. 7), and nonlinearities in material properties from the formulations will then have a larger effect on predictions in the horizontal weir. Interestingly, removal of the blend with the higher proportion of dense



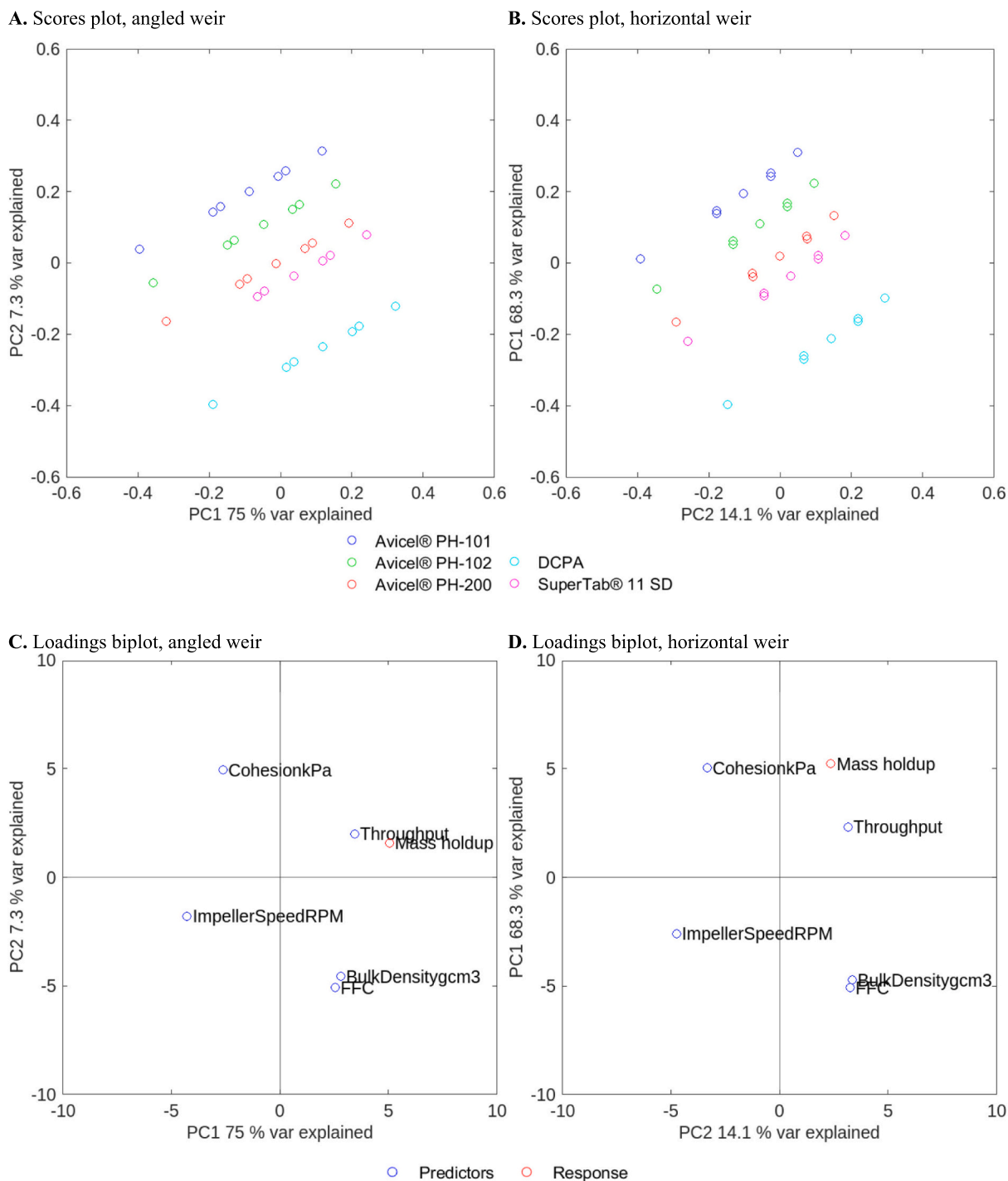


Fig. 6. Scores plots for the angled (A) and horizontal (B) weirs, and predictor/response loadings plots for the angled and horizontal (D) weirs. For the horizontal weir (B, D) principal component 2 has been placed on the x-axis as it has the highest variance of the response explained, and the manner in which it treats the predictors is similar to the case of the angled weir PC1. For the loadings plot, in the lower right quadrant are bulk density, and FFC.

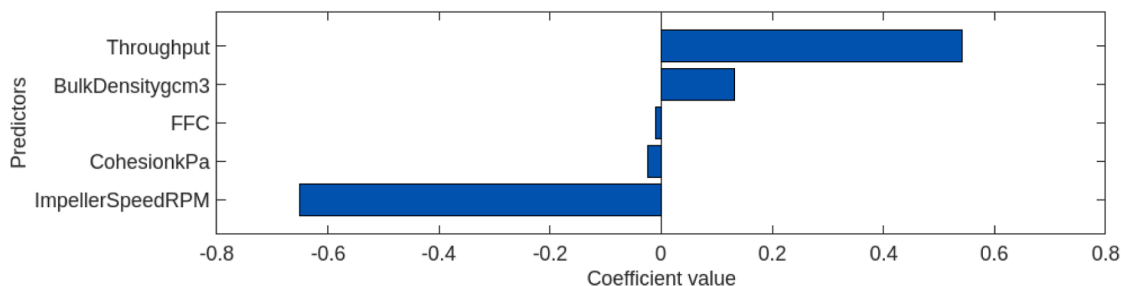
material (blend 3, which is 39 % DCPA, Table 2) dramatically improves results for the horizontal wear, leading to  $R^2$  and RMSE values of 0.82 and 0.247 kg, respectively (for the angled weir there is little change, with  $R^2$  and RMSE values of 0.416 and 0.244 kg). DCPA not only has high bulk and tapped densities but also has an extremely high true density (Table 1). Another potential predictor that was explored at this stage was compressibility, characterized via the Carr's Compressibility Index:

$$CI = \frac{\rho_{tapped} - \rho_{bulk*}}{\rho_{tapped}} \cdot 100 \tag{4}$$

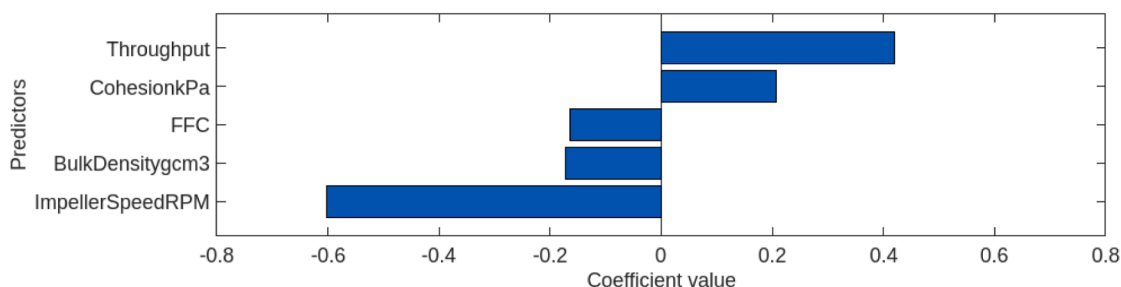
A high  $CI$  value corresponds to a more compressible powder, and a low  $CI$  value corresponds to a comparatively incompressible powder. Inclusion of  $CI$  as a predictor in the PLS approach did not however meaningfully change the PLS model outcomes – it is thought the other predictors of cohesion and flow function coefficient (often well correlated with compressibility) can account for much of the variance in the data.

Given the number of pure components and blends used in the study, and the fact that two weir geometries are used, extending conclusions to e.g. all weir geometries (or even no weir) is challenging. Furthermore, it

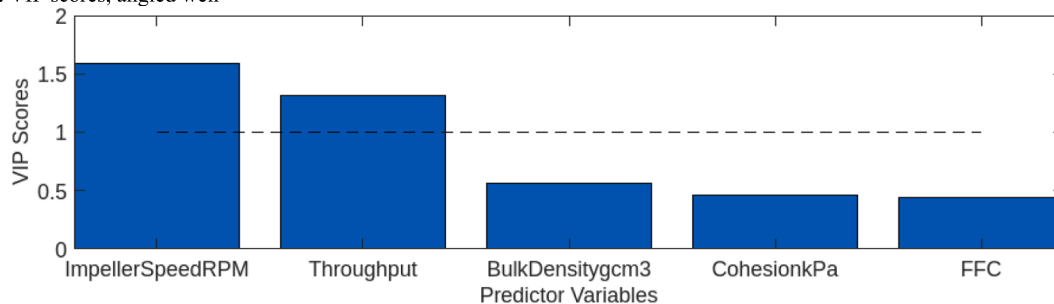
A. Predictor coefficients, angled weir



B. Predictor coefficients, horizontal weir



C. VIP scores, angled weir



D. VIP scores, horizontal weir

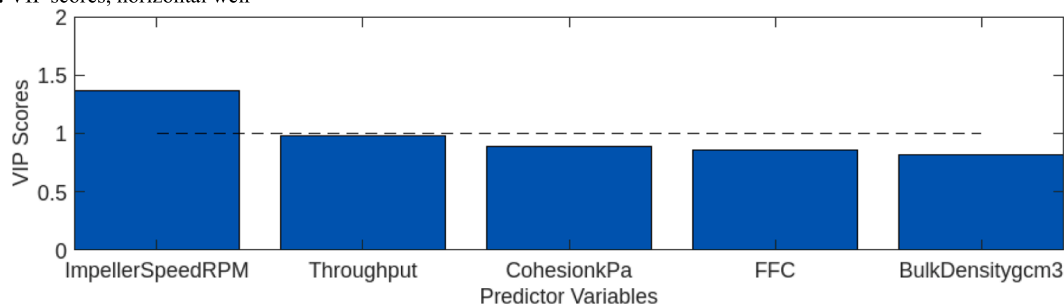


**Fig. 7.** Predictor coefficients for the angled and horizontal weirs (A and B, respectively) and Variable Importance in Projection (VIP) scores for angled and horizontal weirs (C and D, respectively). Coefficients are the direct numerical relation between predictors and the response as determined by the PLS model, while VIP scores give an overall view of the relative importance of each predictor considering all principal components and include weighting for the amount of response variance explained by each component.

is entirely possible that there are nonlinear trends that cause the observed phenomena (whether how the material properties of blends compare to their pure components or how bulk powders of different properties respond to blender operation), which PLS by its very nature cannot accurately capture. However, in the cases of real formulations the material properties in question will be mixtures and not the extremes of pure components, and a pragmatic model may not need to span a very broad material property space. Ultimately, the clear difference in how the angled and horizontal weirs affect mass holdup underscore how an appropriate data-driven approach (such as that used by Jones-Salkey and co-workers [15]) built using a comprehensive dataset could be a

high-utility tool towards assisting equipment configuration and process set-up decisions.

### 3.3. Summary and overview

It is clear that the two weir geometries – angled aperture and horizontal aperture – perform differently, although different outcomes can be seen depending on impeller speed and material properties. Key observations can be summarised as follows:

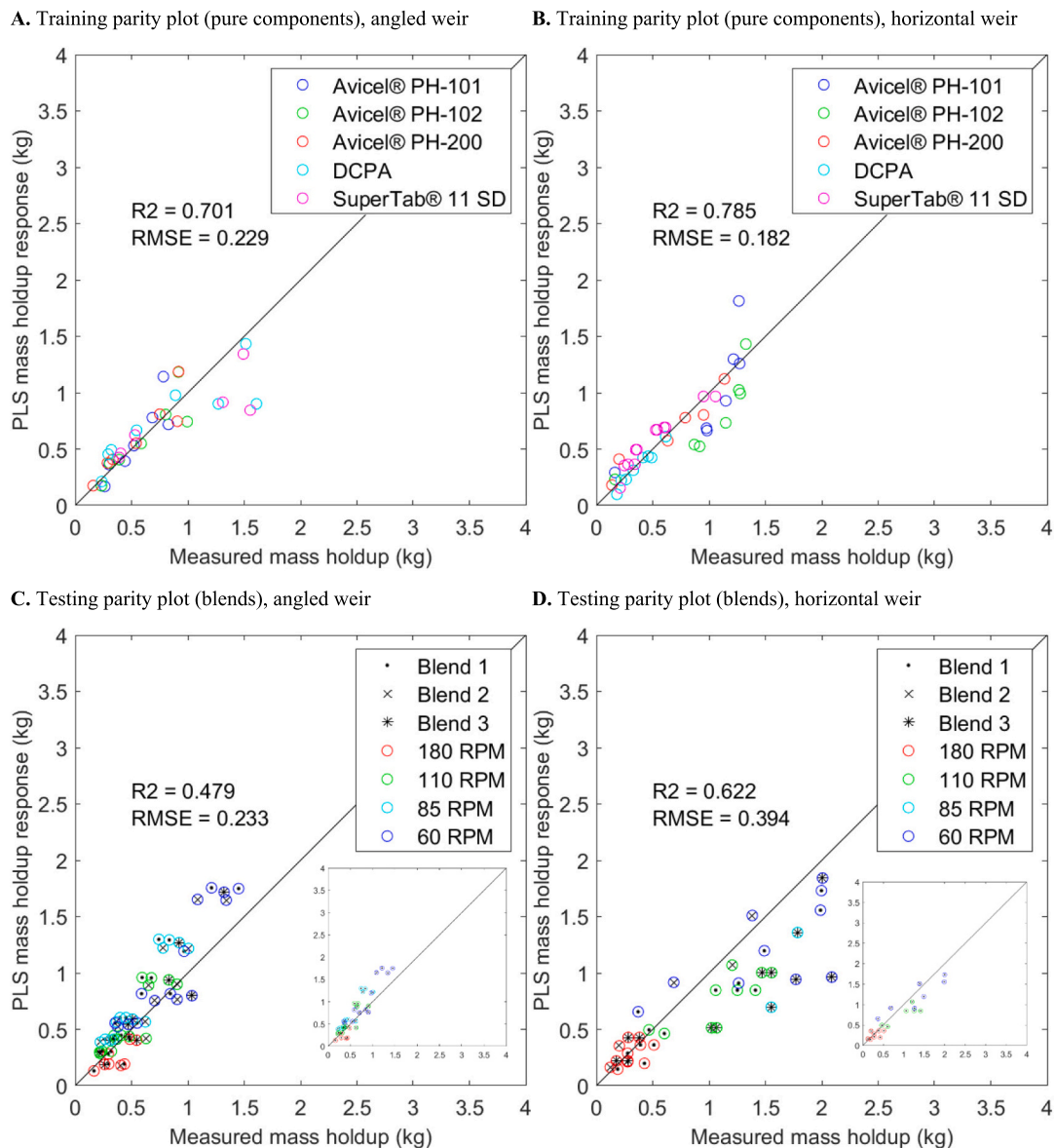


**Fig. 8.** Parity plots for the training sets using pure components (A, angled weir; B, horizontal weir), and parity plots for the test sets using blends (C, angled weir; D, horizontal weir). In the training plots (A, B) colours indicated materials, and in the test plots (C, D) colours indicate impeller speed. Inset plots in C and D are with blend 3 removed.

- Mass holdup increases with throughput as observed for different single materials and blends, and decreases with impeller speed. The weir which results in higher holdup depends on material properties: bulk density and flowability. Impeller speed becomes the dominant variable when it is high, and mass holdup no longer changes with material properties, likely due to powder fluidisation or annular behaviour from centrifugal forces.
- Mean residence time (Eq. (3)) decreases with increasing throughput and impeller speed, and curvature and magnitude of the decrease depends on weir and material properties specifically.
- Based on the relevant properties identified during this study it is hypothesised that material properties of bulk density, flowability, and cohesion influence the relative alignment of the bulk powder surface to the outlet weir. An increased residence mass occurs where the inclination of the powder bed surface is similar to the angle of the outlet weir.

#### 4. Conclusions

The present work highlights the interplay between various key factors (mass throughput, impeller speed, outlet weir geometry, and material properties) relevant to the mass holdup performance of a continuous screw blender. Use of a weir with a horizontal aperture at the outlet allows for greater mass holdup, but this is dependent on material properties – materials with higher densities and lower cohesion exhibit greater mass holdup when angled apertures are used. This is likely due to whether the bulk powder can form an angled surface, with a surface that matches the angle of the outlet aperture (determined by weir choice) leading to higher mass holdup. The present work underscores the need for understanding of process phenomena that may fundamentally differ not just between materials but also choice of equipment configuration.

#### Nomenclature

*c* Cohesion (kPa)

<i>CI</i>	Compressibility Index (–)
<i>E</i>	Exit age distribution curve (–)
<i>M</i>	Mass holdup (kg)
$\dot{m}$	Mass throughput (kg)
<i>t</i>	Time (s)
<i>MPS</i>	Major principal stress (kPa)
<i>UFS</i>	Unconfined failure strength (kPa)
$\rho_{bulk}$	Bulk density (g cm <sup>-3</sup> )
$\rho_{tapped}$	Tapped density (g cm <sup>-3</sup> )
$\varphi'$	Effective angle of internal friction (°)
$\tau$	Mean residence time (s)
$\tau_{mass}$	Mean residence time (calculated from mass throughput and mass holdup) (s)
$\omega$	Rotation rate (s <sup>-1</sup> )

### CRedit authorship contribution statement

**Hikaru Graeme Jolliffe:** Writing – review & editing, Writing – original draft, Visualization, Validation, Methodology, Formal analysis, Data curation. **Maria A. Velazco-Roa:** Writing – original draft, Formal analysis, Data curation. **Luis Martin de Juan:** Writing – review & editing, Formal analysis, Conceptualization. **Martin Prostredny:** Writing – review & editing, Methodology, Investigation, Data curation. **Carlota Mendez Torrecillas:** Writing – review & editing, Methodology, Investigation, Formal analysis, Data curation, Conceptualization. **Gavin Reynolds:** Writing – review & editing, Supervision, Formal analysis, Conceptualization. **Deborah McElhone:** Supervision, Resources, Project administration. **John Robertson:** Writing – review & editing, Supervision, Resources, Methodology, Investigation, Funding acquisition, Conceptualization.

### Declaration of competing interest

The authors declare that they have no known competing financial interests or personal relationships that could have appeared to influence the work reported in this paper.

### Acknowledgements

This work has been funded by the Medicines Manufacturing Innovation Centre project (MMIC), UK (project ownership: Centre for Process Innovation, CPI). Funding has come from Innovate UK and Scottish Enterprise. Founding industry partners with significant financial and technical support are AstraZeneca and GSK. The University of Strathclyde (via CMAC) is the founding academic partner. Pfizer are project partners and have provided key technical input and data. Project partners DFE Pharma (special thanks to Sara Fathollahi) have provided materials and technical input, and project partners Gericke AG (special thanks to Bernhard Meir) have provided technical equipment support and advice. Project partners Siemens and Applied Materials have provided key software expertise.

### Appendix A. Supplementary data

Supplementary data to this article can be found online at <https://doi.org/10.1016/j.powtec.2024.120440>.

### Data availability

Data will be made available on request.

### References

- [1] B. Bekaert, W. Grymonpré, A. Novikova, C. Vervaet, V. Vanhoorne, Impact of blend properties and process variables on the blending performance, *Int. J. Pharm.* 613 (2022) 121421, <https://doi.org/10.1016/j.ijpharm.2021.121421>.
- [2] B. Bekaert, B. Van Snick, K. Pandelaere, J. Dhondt, G. Di Pretoro, T. De Beer, C. Vervaet, V. Vanhoorne, Continuous direct compression: development of an empirical predictive model and challenges regarding PAT implementation, *Int. J. Pharma. X* 4 (2022) 100110, <https://doi.org/10.1016/j.ijpx.2021.100110>.
- [3] C.L. Burcham, A.J. Florence, M.D. Johnson, Continuous manufacturing in pharmaceutical process development and manufacturing, *Annu. Rev. Chem. Biomol. Eng.* 9 (2018) 253–281, <https://doi.org/10.1146/annurev-chembioeng-060817-084355>.
- [4] P.V. Danckwerts, Continuous flow systems: distribution of residence times, *Chem. Eng. Sci.* 2 (1953) 1–13, [https://doi.org/10.1016/0009-2509\(53\)80001-1](https://doi.org/10.1016/0009-2509(53)80001-1).
- [5] M.E.E. Davis, R.J.J. Davis, *Fundamentals of Chemical Reaction Engineering*, Courier Corporation, 2012.
- [6] A. Domokos, B. Nagy, B. Szilágyi, G. Marosi, Z.K. Nagy, Integrated continuous pharmaceutical technologies—a review, *Org. Process. Res. Dev.* 25 (2021) 721–739, <https://doi.org/10.1021/acs.oprd.0c00504>.
- [7] A. Dubey, A. Sarkar, M. Ierapetritou, C.R. Wassgren, F.J. Muzzio, Computational approaches for studying the granular dynamics of continuous blending processes, 1 – DEM based methods, *Macromol. Mater. Eng.* 296 (2011) 290–307, <https://doi.org/10.1002/mame.201000389>.
- [8] A. Dubey, A.U. Vanarase, F.J. Muzzio, Impact of process parameters on critical performance attributes of a continuous blender—a DEM-based study, *AIChE J.* 58 (2012) 3676–3684, <https://doi.org/10.1002/aic.13770>.
- [9] M.S. Escotet-Espinoza, S. Moghtadernejad, S. Oka, Y. Wang, A. Roman-Ospino, E. Schäfer, P. Cappuyns, I. Van Assche, M. Futran, M. Ierapetritou, F. Muzzio, Effect of tracer material properties on the residence time distribution (RTD) of continuous powder blending operations. Part I of II: Experimental evaluation, *Powder Technol.* 342 (2019) 744–763, <https://doi.org/10.1016/j.powtec.2018.10.040>.
- [10] M.S. Escotet-Espinoza, S. Moghtadernejad, S. Oka, Z. Wang, Y. Wang, A. Roman-Ospino, E. Schäfer, P. Cappuyns, I. Van Assche, M. Futran, F. Muzzio, M. Ierapetritou, Effect of material properties on the residence time distribution (RTD) characterization of powder blending unit operations. Part II of II: Application of models, *Powder Technol.* 344 (2019) 525–544, <https://doi.org/10.1016/j.powtec.2018.12.051>.
- [11] Y. Gao, F.J. Muzzio, M.G. Ierapetritou, A review of the residence time distribution (RTD) applications in solid unit operations, *Powder Technol.* 228 (2012) 416–423, <https://doi.org/10.1016/j.powtec.2012.05.060>.
- [12] Y. Gao, A. Vanarase, F. Muzzio, M. Ierapetritou, Characterizing continuous powder mixing using residence time distribution, *Chem. Eng. Sci.* 66 (2011) 417–425, <https://doi.org/10.1016/j.ces.2010.10.045>.
- [13] M. Jaspers, T.P. Roelofs, A. Lohrmann, F. Tegel, M.K. Maqsood, Y.L. Song, B. Meir, R. Elkes, B.H.J. Dickhoff, Process intensification using a semi-continuous mini-blender to support continuous direct compression processing, *Powder Technol.* 428 (2023) 118844, <https://doi.org/10.1016/j.powtec.2023.118844>.
- [14] A.W. Jenike, *Storage and Flow of Solids* 53, *Bulletin of the University of Utah*, 1964.
- [15] O. Jones-Salkey, C.R.K. Windows-Yule, A. Ingram, L. Stahler, A.L. Nicusan, S. Clifford, L. Martin de Juan, G.K. Reynolds, Using AI/ML to predict blending performance and process sensitivity for continuous direct compression (CDC), *Int. J. Pharm.* 651 (2024) 123796, <https://doi.org/10.1016/j.ijpharm.2024.123796>.
- [16] E.B. Nauman, Residence time theory, *Ind. Eng. Chem. Res.* 47 (2008) 3752–3766, <https://doi.org/10.1021/ie071635a>.
- [17] J.G. Osorio, F.J. Muzzio, Effects of processing parameters and blade patterns on continuous pharmaceutical powder mixing, *Chem. Eng. Process. Process Intensif.* 109 (2016) 59–67, <https://doi.org/10.1016/j.cep.2016.07.012>.
- [18] J. Palmer, G.K. Reynolds, F. Tahir, I.K. Yadav, E. Meehan, J. Holman, G. Bajwa, Mapping key process parameters to the performance of a continuous dry powder blender in a continuous direct compression system, *Powder Technol.* 362 (2020) 659–670, <https://doi.org/10.1016/j.powtec.2019.12.028>.
- [19] K. Plumb, Continuous processing in the pharmaceutical industry - changing the mind set, *Chem. Eng. Res. Des.* 83 (2005) 730–738, <https://doi.org/10.1205/cherd.04359>.
- [20] P.M. Portillo, M.G. Ierapetritou, F.J. Muzzio, Effects of rotation rate, mixing angle, and cohesion in two continuous powder mixers—a statistical approach, *Powder Technol.* 194 (2009) 217–227, <https://doi.org/10.1016/j.powtec.2009.04.010>.
- [21] P.M. Portillo, M.G. Ierapetritou, F.J. Muzzio, Characterization of continuous convective powder mixing processes, *Powder Technol.* 182 (2008) 368–378, <https://doi.org/10.1016/j.powtec.2007.06.024>.
- [22] P.M. Portillo, A.U. Vanarase, A. Ingram, J.K. Seville, M.G. Ierapetritou, F.J. Muzzio, Investigation of the effect of impeller rotation rate, powder flow rate, and cohesion on powder flow behavior in a continuous blender using PEPT, *Chem. Eng. Sci. Pharm. Eng. Sci. A Key Tomorrow's Drugs* 65 (2010) 5658–5668, <https://doi.org/10.1016/j.ces.2010.06.036>.
- [23] S.D. Schaber, D.I. Gerogiorgis, R. Ramachandran, J.M.B. Evans, P.I. Barton, B. L. Trout, Economic analysis of integrated continuous and batch pharmaceutical manufacturing: a case study, *Ind. Eng. Chem. Res.* 50 (2011) 10083–10092, <https://doi.org/10.1021/ie2006752>.
- [24] U.K. Medicines & Healthcare products Regulatory Agency, *British Pharmacopoeia Appendix XVII S. Bulk Density and Tapped Density of Powders*, *British Pharmacopoeia*, 2023.
- [25] U.S. FDA, PAT — A Framework for Innovative Pharmaceutical Development, Manufacturing, and Quality Assurance [WWW Document], URL, <https://www.fda.gov/regulatory-information/search-fda-guidance-documents/pat-framework-innovative-pharmaceutical-development-manufacturing-and-quality-assurance>, 2023 (accessed 4.4.24).

- [26] U.S. FDA, Q8(R2) Pharmaceutical Development [WWW Document], URL, <https://www.fda.gov/regulatory-information/search-fda-guidance-documents/q8-r2-pharmaceutical-development>, 2020 (accessed 4.4.24).
- [27] A.U. Vanarase, F.J. Muzzio, Effect of operating conditions and design parameters in a continuous powder mixer, *Powder Technol.* 208 (2011) 26–36, <https://doi.org/10.1016/j.powtec.2010.11.038>.
- [28] A.U. Vanarase, J.G. Osorio, F.J. Muzzio, Effects of powder flow properties and shear environment on the performance of continuous mixing of pharmaceutical powders, *Powder Technol.* 246 (2013) 63–72, <https://doi.org/10.1016/j.powtec.2013.05.002>.
- [29] C. Zheng, L. Li, B.J. Nitert, N. Govender, T. Chamberlain, L. Zhang, C.-Y. Wu, Investigation of granular dynamics in a continuous blender using the GPU-enhanced discrete element method, *Powder Technol.* 412 (2022) 117968, <https://doi.org/10.1016/j.powtec.2022.117968>.